

Particle swarm optimization and finite-difference time-domain algorithms for gas sensors based on photonic crystal fiber

ZAHRA DASHTBAN¹, MANSOOR BAGHERI², MOHAMMAD ALI ALAVIANMEHR¹,
SONBOLEH SALIMI³

¹Department of Electrical and Electronic Engineering, Shiraz University of Technology, Shiraz, IRAN.

²Pergas Payam Parseh Company, Tehran, IRAN

³Faculty of Technology, Art and Design (TKD), Oslo Metropolitan University, Oslo, NORWAY

Abstract: In this paper, a gas detection sensor based on photonic crystal fibers with high sensitivity and low loss is designed and optimized for the detection of two gases, namely carbon tetrachloride (CCl_4 , $n=1.461$) and tin tetrachloride (SnCl_4 , $n = 1.5086$). The finite-difference time-domain (FDTD) method is used to simulate light propagation in the PCF. By applying the PSO algorithm and optimizing the geometric dimensions of the photonic crystal fiber, including the core diameter, hole diameter, and lattice constant, very low losses are achieved, resulting in higher relative sensitivity. The numerical simulation results demonstrate that the designed sensor has a sensitivity coefficient of 70.2% and 77.3% for CCl_4 and SnCl_4 at a wavelength of 2.6 μm , respectively. It also exhibits very low losses (in the range of 10^{-8} dB/cm) compared to other studies. This sensor is a suitable tool for detecting toxic gases in industries such as chemical manufacturing, environmental monitoring, and occupational health and safety, with absorption in the spectral range of the bandgap from 1 to 3 μm .

Key-Words: Photonic Crystal Fiber (PCF), Gas sensor, FDTD Numerical Method, Particle Swarm Optimization (PSO), Relative Sensitivity, confinement loss.

Tgegkxgf <Cr tkf33."42460Tgxkuf <P qxgo dgt"3; . "42460Ceegr vgf <F gego dgt"49."42470Rwdrkuj gf <O ctej "53."42470'

1 Introduction

As Photonic crystal fibers are used to design sensors for detecting gases and substances based on their absorption spectrum. In recent years, gas sensors have gained significant traction across diverse sectors, including metallurgy, chemical industries, petroleum, steel production, mining, environmental protection, and aerospace. This trend has established gas sensors as a prominent subject within the field of sensor technology.[1], [2]. The advancement of industrial automation and artificial intelligence has created an urgent need for technical progress in detecting gas concentration and composition for rapid gas leak and explosion warnings [3]. Optical spectrum-based gas sensors have features such as intrinsic safety, high sensitivity, and excellent detection capabilities. Researchers have proposed various structures for both hollow-core and solid-core photonic crystal fibers designed for sensing applications. Significant efforts have been made to enhance the sensitivity coefficient by modifying the physical structure of these fibers.[4]– [7]. Numerical results indicate that the sensitivity coefficient for solid-core structures is not significantly high, which is a disadvantage of these fibers for sensing applications. The excellent characteristics of hollow-core microstructured fibers have made them one of the best candidates for fiber-optic sensors. By

tuning the fiber-optic structure to have the maximum interaction with the sensing material, the relative sensitivity of the structure can be significantly improved.

Recently, Rabee *et al.* [8] presented a Spiral PCF gas sensor to achieve high relative sensitivity for liquid and chemical sensing applications. They demonstrated that the relative sensitivity achieved for the optimized parameters are 56.8%, 58.3%, and 62.7% for water ($n=1.33$), propane ($n=1.34$), and propylene ($n=1.36$), respectively. The simulation results indicated a relative sensitivity of 27% and a loss of 0.034 dB/m at a wavelength of $\lambda = 5 \mu\text{m}$. Molaieifard *et al.* presented a photonic crystal fiber with a hexagonal structure for gas sensing. They showed that a relative sensitivity of 67.07% and a loss of 3.2×10^{-3} dB/m at a wavelength of 1.578 μm were achieved [9]. Additionally, a photonic crystal structure was proposed both vertically and horizontally (H-PCF and V-PCF) for sulfur dioxide (SO_2) sensing [10]. The highest sensitivity of this structure was obtained at a wavelength of 1 μm for the V-PCF structure. Their results showed that the relative sensitivity of the mentioned structure for SO_2 sensing was 34.59%. Hossain *et al.* [11] introduced a square-core photonic crystal fiber (PCF) for petrochemical sensing, with its performance rigorously evaluated numerically

across the frequency range of 1.2 to 3.8 THz. This sensor exhibits a remarkable relative sensitivity of approximately 97% and a minimal confinement loss of 10^{-14} cm^{-1} at 3.7 THz. Dashtban *et al.* presented a PCF sensor featuring rectangular air holes and constructed from Zeonex material for detecting ethanol, methanol, and propanol within the 3 to 5 THz range [12]. This sensor demonstrates high relative sensitivities, achieving up to 79.3% for propanol, and exhibits near-zero confinement loss, thereby outperforming existing designs.

This paper presents the design of a high-sensitivity, low-loss quasi-crystal structure intended for detecting a variety of gases., including CCl_4 and SnCl_4 , in the MIR range. By pumping the optical spectrum into the mid-infrared region at the sensor's input, the relative sensitivity of the structure can be enhanced, as the absorption of many gases and even liquids in the mid-infrared region is several times higher. The increased light absorption by gases in this region leads to more accurate gas identification. Then the geometric dimensions of the structure, such as the core diameter, pitch, and the diameter of the air holes in the cladding, have been optimized using the PSO algorithm to achieve high sensitivity. Optimization algorithms play a crucial role in enhancing the performance of photonic crystal fiber (PCF) sensors by refining their design and operation for specific sensing applications. These sensors, which leverage the unique properties of PCFs, such as their ability to confine light in photonic band gaps, offer significant advantages in terms of sensitivity, bandwidth, and miniaturization. However, to fully harness their potential, optimization techniques are required to fine-tune their geometrical parameters (e.g., hole diameter, pitch, fiber length) and operational conditions (e.g., wavelength, refractive index).

The bandgap of the designed structure has been determined utilizing the plane wave expansion method. Then, the linear and nonlinear profiles obtained from the numerical results based on the FDTD method, including the refractive index, scattering, loss, effective cross-section, nonlinear parameter γ , and relative sensitivity for the designed structure, have been computed. It has been shown that the sensitivity of 70.2% and 78.2% for CCL_4 and SnCl_4 at a wavelength of $2.6 \mu\text{m}$, respectively.

2 Structure Design and Numerical analysis of optical properties

Fig. 1 shows a cross-section of a hollow-core photonic crystal fiber and the electric field intensity distribution profile for both TM and TE modes for sensing purposes. The fiber consists of magnesium

fluoride (MgF_2) and has air holes surrounding the core, arranged in a quasi-crystalline structure. Magnesium fluoride (MgF_2) is used as the material

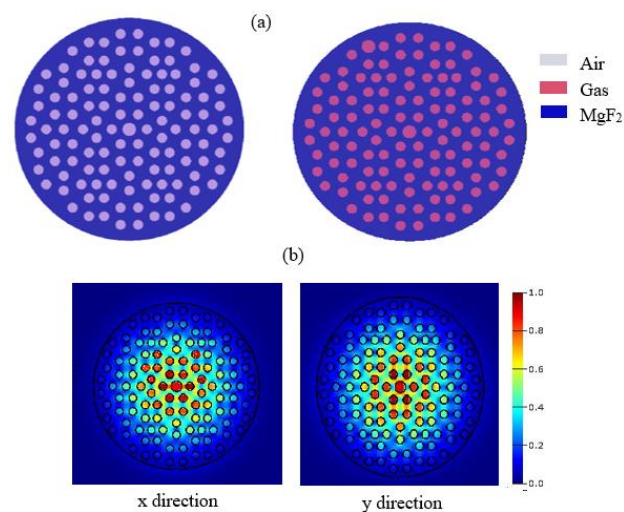


Fig. 1. (a) The cross-section of the gas sensor PCF proposed in this study without gas and the gas-filled state. (b) Modal intensity distribution along x direction along y direction a $2.5 \mu\text{m}$.

for the photonic crystal fiber to ensure a desirable effective refractive index for cladding by selecting large air hole diameters (to enhance the sensitivity coefficient).

The designed quasi-photonic crystal fiber has a symmetry order of 12, meaning the air holes in this lattice are randomly arranged in a geometric pattern of squares and parallelograms, with a lattice constant of $2 \mu\text{m}$. Using the plane wave expansion method, the band has been calculated. The proposed structure has a relatively wide photonic bandgap in the wavelength range of 1 to $3 \mu\text{m}$.

3 Particle swarm optimization (PSO) algorithm

The optimization of the dimensions of the proposed photonic crystal fiber is performed using a particle swarm optimization algorithm, which is a population-based random optimization method. This technique can be applied to problems whose solutions are points or surfaces in an n-dimensional space. In such a space, hypotheses are made, and an initial velocity is assigned to them. Furthermore, the communication channels among particles are taken into account. Subsequently, these particles navigate through the solution space, and the outcomes are evaluated based on a defined 'fitness criterion' after each time interval. Over time, the particles exhibit an accelerate towards those with superior fitness criteria that are part of the same communication group. Although each method works well within a range of problems, this approach is an ideal solution

for solving continuous optimization problems. In this paper, the initial population is formed by three parameters: core radius (rc), air hole radius (d), and

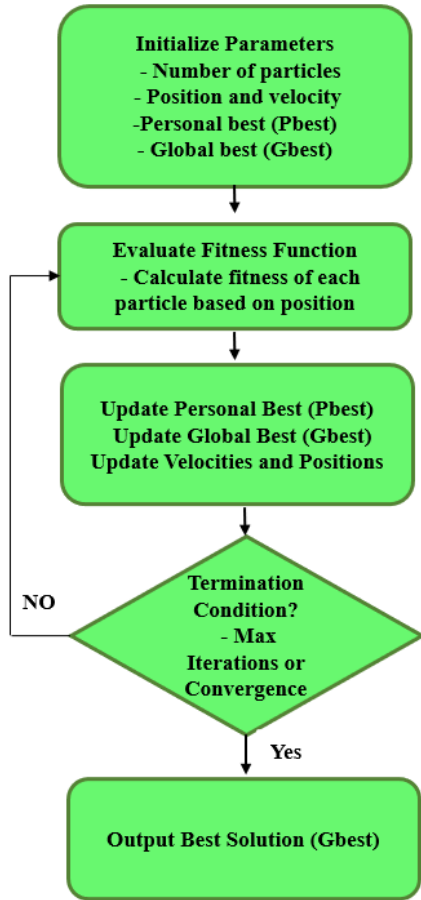


Fig. 2. The block diagram of the fiber dimension optimization process with the PSO algorithm.

lattice constant (Λ). The goal is to achieve high sensitivity and low loss at a wavelength of 1 to 3 μm .

The optimal parameters, which include the core radius, air hole diameter, and lattice constant, are derived from the algorithm's output. The optimization results utilizing the PSO algorithm indicate that the photonic crystal fiber with a core radius of 1.275 μm , an air hole radius of 1.2 μm , and a lattice constant of 2.5 μm possesses the most favorable dimensions.

4 Results and analysis

The structure illustrated in Fig. 1 is modeled using the finite-difference time-domain (FDTD) method. The Sellmeier equation for the refractive index of magnesium fluoride as a function of wavelength (λ) is written as follows [13]:

$$n(\lambda) = \left\{ 1 + 0.4875\lambda^2(\lambda^2 - 0.04338^2)^{-1} + 0.3987\lambda^2(\lambda^2 - 0.0946^2)^{-1} + 2.312\lambda^2(\lambda^2 - 23.79^2)^{-1} \right\}^{1/2} \quad (1)$$

The effective refractive index of the fiber at each wavelength is calculated using the finite-difference time-domain (FDTD) numerical method. This study presents the real and imaginary components of the effective refractive index for the proposed hollow-core photonic crystal fiber, illustrated as a function of wavelength in Figs 3 and 4.

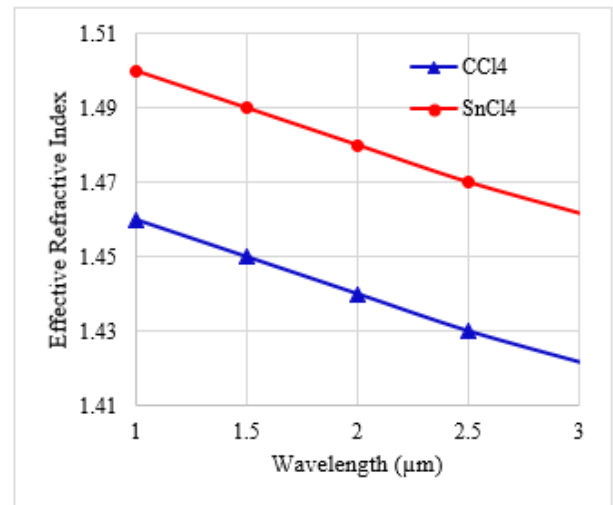


Fig3. The variation of the real parts of the effective refractive index for the proposed PCF gas sensor in relation to wavelength.

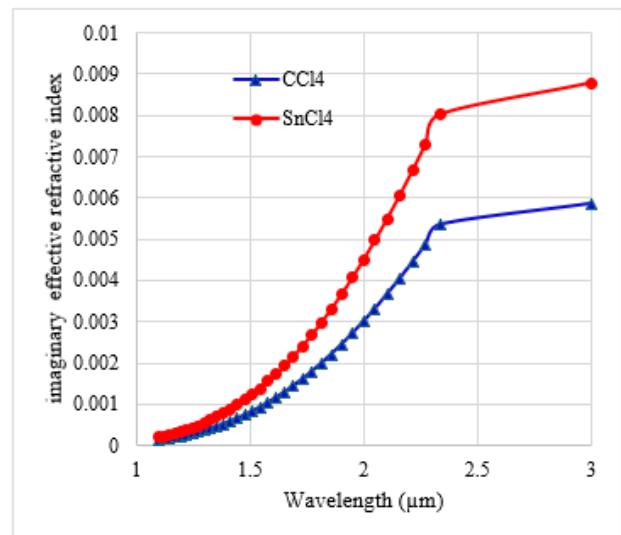


Fig. 4. Variation of the imaginary parts of the effective refractive index with wavelength for the proposed PCF gas sensor.

By calculating the real part of the refractive index ($\text{Re}[n_{\text{eff}}]$) of the designed photonic crystal fiber, the

total dispersion (chromatic dispersion), which is the sum of waveguide dispersion ($D_w(\lambda)$) and material dispersion ($D_M(\lambda)$), is calculated at each wavelength using the following equation. The results are plotted in Fig. 5 [14].

$$D(\lambda) = D_w(\lambda) + D_M(\lambda) = -\frac{\lambda}{c} \frac{d^2}{d\lambda^2} \text{Re}[n_{\text{eff}}(\lambda)] \quad (2)$$

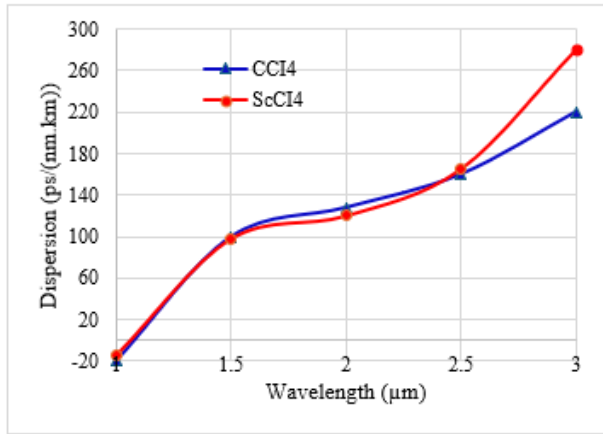


Fig. 5. Variation of dispersion profile with wavelength for the proposed PCF gas sensor.

The losses of the structure depend on the arrangement of the circular air holes in either a square or hexagonal pattern, their diameter, the lattice constant, and similar parameters. By optimizing the structure to enhance the effective cross-sectional area of the fiber, it is possible to minimize losses. The losses of the structure also depend on the core diameter, the arrangement of the circular air holes (in square, hexagonal, or circular patterns in the proposed design), the diameter of the holes, and the lattice constant. The structure's losses at each wavelength are calculated using the following equation [13]:

$$L_c(\lambda) = 8.686k_0 \text{Im}[n_{\text{eff}}(\lambda)] \quad (3)$$

$\text{Im}[n_{\text{eff}}(\lambda)]$ is the imaginary part of the refractive index as a function of wavelength, K_0 , the wave number in free space, is equal to Fig 4. Fig 6 illustrates the total losses, encompassing both material and waveguide losses, for both the non-optimized and optimized structures.

As shown in Fig 6, with increasing wavelength and rc , the fiber losses increase because, as the wavelength increases, the mode area enlarges, and the optical field extends into the cladding, losing its energy.

The influence of linear and nonlinear parameters on light propagation within optical fibers is significant. The linear component is represented by loss and dispersion. The effective mode area is a vital parameter in the design of photonic crystal fibers, as it reflects the degree to which the mode is confined

within the core. Therefore, it is closely related to the core size and doping levels.

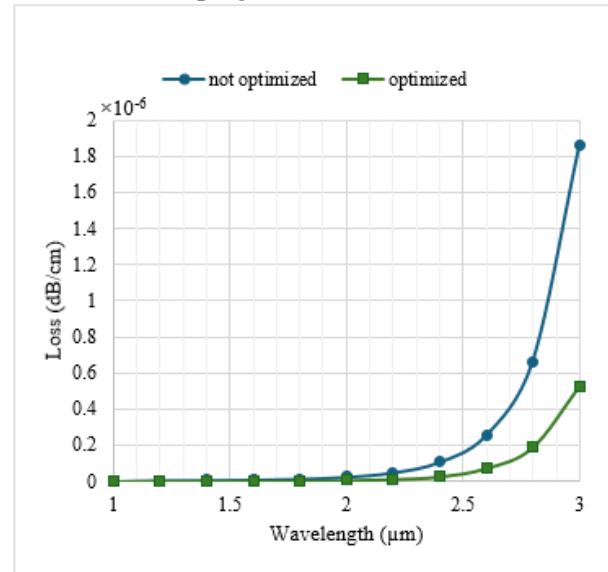


Fig. 6. Variation of Confinement loss with wavelength for the proposed PCF gas sensor for $d=2.4\mu\text{m}$, $rc=1.275\mu\text{m}$, $\Lambda=2.5\mu\text{m}$ (optimized with PSO), and $d=2.2\mu\text{m}$, $rc=1.5\mu\text{m}$, $\Lambda=2.3\mu\text{m}$ (Before optimization).

The effective mode area A_{eff} can be calculated using the following formula [13]:

$$A_{\text{eff}}(\lambda) = \frac{\left(\int_{-\infty}^{+\infty} \int_{-\infty}^{+\infty} |F(x,y)|^2 dx dy \right)^2}{\int_{-\infty}^{+\infty} \int_{-\infty}^{+\infty} |F(x,y)|^4 dx dy} \quad (4)$$

Where $F(x,y)$ is the amplitude of the transverse electric field propagating inside the fiber. The effective mode area (A_{eff}) for the proposed structure at each wavelength for the fundamental mode is calculated, and the results are presented in Fig. 7.

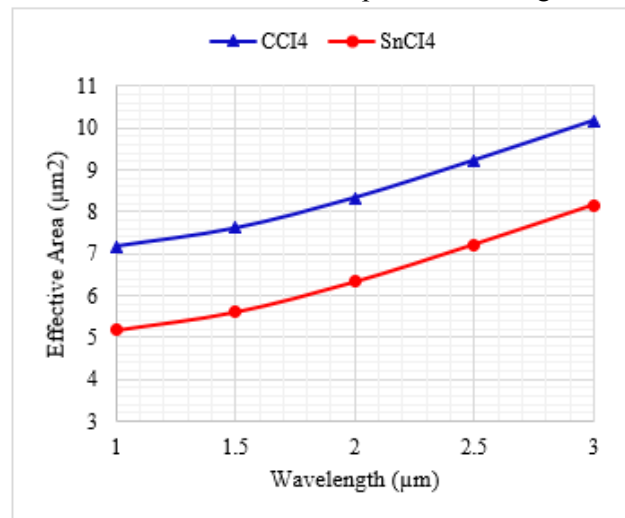


Fig. 7. Variation of Effective area with wavelength for the proposed PCF gas sensor for CCl₄ and SnCl₄.

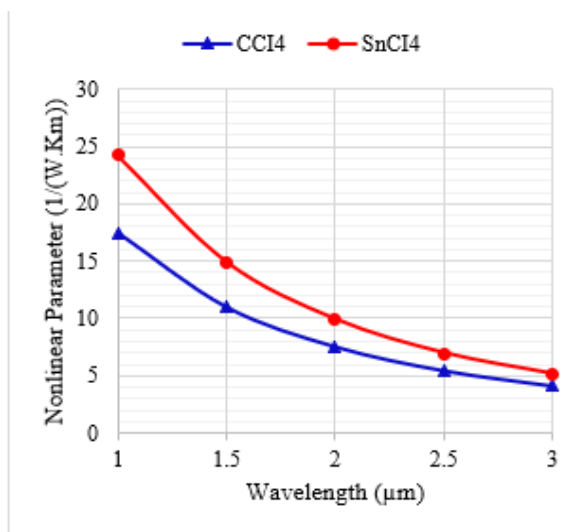


Fig. 8. Nonlinear coefficient of the proposed PCF gas sensor in terms of wavelength for CCl₄ and SnCl₄.

As seen in Fig. 7, the effective mode area at a wavelength of 2.5 μm is 9.22 and 7 μm² for CCl₄ and SnCl₄, respectively.

The nonlinear coefficient γ at the central frequency ω_0 is computed according to the following equation [15]:

$$\gamma (\text{W} \cdot \text{m})^{-1} = n_2 \omega_0 / c A_{\text{eff}} (\lambda) \quad (5)$$

n_2 is the nonlinear refractive index of the material. The nonlinear coefficient γ is calculated based on the effective cross-sectional area at each wavelength for the proposed structure, as outlined in equation (5). The nonlinear coefficient profile as a function of wavelength for the proposed structure is computed and shown in Fig. 8.

As shown in fig. 8, the nonlinear coefficients at a wavelength of 2.5 μm are 5.4 and 6.96 w⁻¹ Km⁻¹ for CCl₄ and SnCl₄, respectively. As mathematically expected, the effective mode area and nonlinear coefficient are inversely related. An increase in wavelength leads to a larger mode area, which in turn results in a decrease in the nonlinear coefficient.

4 Relative sensitivity of proposed PCF

In this paper, as shown in Fig. 9, the relative sensitivity coefficient (r) of the proposed PCF gas sensor in its optimized state, for the case where the air holes are filled with CCl₄ and SnCl₄ gas, is computed according to the following equation [16]:

$$r = \frac{n_s}{\text{Re}[n_{\text{eff}}]} f \quad (6)$$

The refractive index of the gas is denoted as n while f represents the fraction of the total optical power contained within the fiber core and other gas-filled holes.

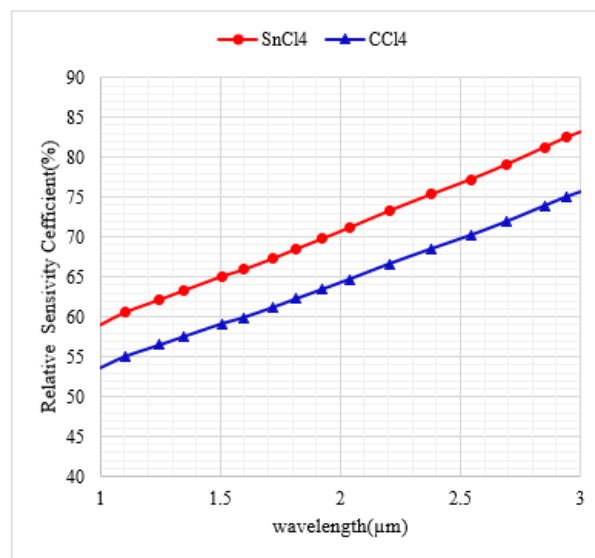


Fig. 9. Variation of Relative sensitivity with wavelength for CCl₄ and SnCl₄.

It can be observed that a relative sensitivity coefficient of 70.2% and 77.3% for CCl₄ and SnCl₄ at a wavelength of 2.6 μm has been achieved. Additionally, the maximum relative sensitivity at a wavelength of 3 μm is 83.21% and 75.6% for SnCl₄ and CCl₄, respectively.

Furthermore, the variation in relative sensitivity with changes in the core radius of the proposed structure, ranging from 1 to 3 μm, has been examined and is shown in Fig. 10(a).

As seen, with an increase in the core radius r_c , the sensitivity coefficient also increases because a larger core radius leads to greater interaction of optical power with the gas molecules. Additionally, an increase in wavelength results in a larger effective mode area, ultimately leading to an increase in the sensitivity coefficient.

The lattice constant is one of the parameters that affect the relative sensitivity. In Fig. 10(b), the effect of lattice constant variations on sensitivity is also examined. The lattice constant of the structure is changed from 2 to 3 μm while keeping the core radius fixed at 1.2 μm, and the relative sensitivity of the structure is plotted at each stage.

As shown in Fig. 10(b), as the lattice constant of the structure decreases, the relative sensitivity of the structure increases. However, it should be noted that reducing the lattice constant also leads to an increase in the confinement losses. When the lattice

constant is reduced to 2 μm , the sensitivity increases to 88.4% at a wavelength of 3 μm . Table 1 highlights the differences between the characteristics of the proposed PCF and those of previously introduced PCFs. The proposed design exhibits high sensitivity and low loss performance, featuring a simple circular ring configuration.

the study reveals that the sensitivity increases with the core radius and wavelength, as these factors facilitate stronger interaction between the optical field and the gas molecules within the fiber. The lattice constant also plays a crucial role in determining the sensitivity, with a decrease in the lattice constant leading to a higher sensitivity,

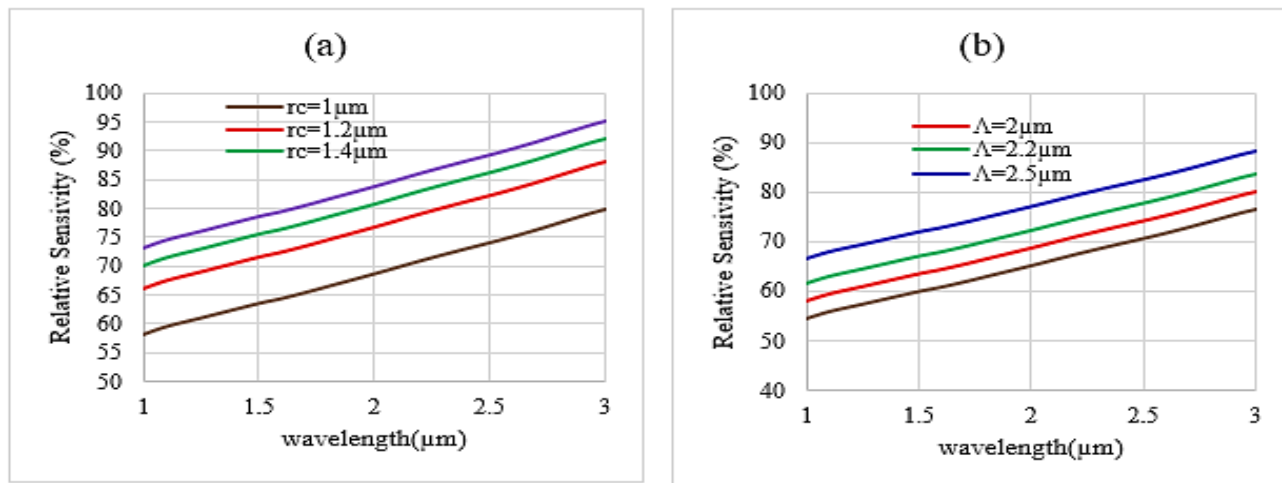


Fig. 10. (a)The variation of Relative sensitivity with respect to changes in the core radius, (b) Relative sensitivity with respect to changes in the lattice constant.

Table1. Comparison of the obtained results with other articles.

	Sensing Object	Wavelength(μm)	Confinement loss(dB/m)	Sensitivity (%)
[17]	H ₂ s/CH ₄	1.33	8.6×10^{-5}	62.7
[18]	Hydrogen cyanide	1.533	1.5×10^{-3}	65.13
[19]	C ₁₀ H ₁₆ /SnCl ₄	1	-----	65.86
[20]	CO	1.567	3.81×10^{-3}	64.28
This Work	SnCl ₄ /CCl ₄	2.6	2×10^{-5}	77.3

4 Conclusion

In this study, the design and optimization of a proposed hollow-core photonic crystal fiber (PCF) for high sensitivity applications have been presented. The FDTD method is employed to simulate the structure numerically. The PSO algorithm was used to optimize the dimensions of the fiber, such as the core radius, air hole diameter, and lattice constant. The results indicate that the fiber's sensitivity is significantly influenced by key parameters such as the core radius, lattice constant, and wavelength. The optimization of these parameters enhances the fiber's performance, achieving a relative sensitivity of maximum relative sensitivity at a wavelength of 3 μm is 83.21% and 75.6% for SnCl₄ and CCl₄, respectively. Moreover,

though at the cost of increased losses. Therefore, having both high relative sensitivity and low confinement losses simultaneously is very important in gas sensors. In many cases, achieving these two characteristics at the same time is challenging, as improving one often leads to the deterioration of the other. In this article, an effort has been made to design the gas sensor so that both high relative sensitivity and low losses are achieved simultaneously by changing the structural features and optimizing the design using the PSO algorithm.

References:

- [1] M. Chintoanu *et al.*, "Methane and carbon monoxide gas detection system based on semiconductor sensor," in *2006 IEEE international conference on automation, quality and testing, robotics*, 2006, vol. 2, pp. 208–211.
- [2] D. B. Papkovsky and R. I. Dmitriev, "Biological detection by optical oxygen sensing," *Chem. Soc. Rev.*, vol. 42, no. 22, pp. 8700–8732, 2013.
- [3] N. Yamazoe and K. Shimanoe, "New perspectives of gas sensor technology," *Sensors Actuators B Chem.*, vol. 138, no. 1, pp. 100–107, 2009.
- [4] J. Sultana, M. S. Islam, K. Ahmed, A.

- Dinovitser, B. W.-H. Ng, and D. Abbott, "Terahertz detection of alcohol using a photonic crystal fiber sensor," *Appl. Opt.*, vol. 57, no. 10, pp. 2426–2433, 2018.
- [5] V. Kaur and S. Singh, "Design approach of solid-core photonic crystal fiber sensor with sensing ring for blood component detection," *J. Nanophotonics*, vol. 13, no. 2, p. 26011, 2019.
- [6] H. Arman and S. Olyaei, "Realization of low confinement loss acetylene gas sensor by using hollow-core photonic bandgap fiber," *Opt. Quantum Electron.*, vol. 53, no. 6, pp. 1–13, 2021.
- [7] H. Arman and S. Olyaei, "Improving the sensitivity of the HC-PBF based gas sensor by optimization of core size and mode interference suppression," *Opt. Quantum Electron.*, vol. 52, no. 9, pp. 1–10, 2020.
- [8] A. S. H. Rabee, M. F. O. Hameed, A. M. Heikal, and S. S. A. Obayya, "Highly sensitive photonic crystal fiber gas sensor," *Optik (Stuttg.)*, vol. 188, pp. 78–86, 2019.
- [9] A. M. Fard, M. J. Sarraf, and F. Khatib, "Design and Optimization of Index Guiding Photonic Crystal Fiber-Based Gas Sensor," *Optik (Stuttg.)*, p. 166448, 2021.
- [10] S. M. Nizar, E. Caroline, and P. Krishnan, "Design and investigation of a high-sensitivity PCF sensor for the detection of sulfur dioxide," *Plasmonics*, pp. 1–11, 2021.
- [11] Hossain, M.B., Křřřz, J., Dhasarathan, V., Rahaman, M.E., 2023. Photonic crystal fiber (PhCF) for petrochemical sensing. *Front. Phys.* 10, 1097841
- [12] Z. Dashtban, S. Ramtinpard, N. Kakesh, and H. Saghaei, "Design and characterization of an ultra-sensitive photonic crystal fiber-based sensor for precise detection of alcohols in the THz regime," *Results in Optics*, vol. 16, p. 100721, Jul. 2024.
- [13] Dashtban, Z., Salehi, M.R., Abiri, E., 2021. Supercontinuum generation in near-and mid-infrared spectral region using highly nonlinear silicon-core photonic crystal fiber for sensing applications. *Photon. Nanostruct.-Fundam. Appl.*, 100942
- [14] M. Ebnali-Heidari, F. Dehghan, H. Saghaei, F. Koochi-Kamali, and M. K. Moravvej-Farshi, "Dispersion engineering of photonic crystal fibers by means of fluidic infiltration," *J. Mod. Opt.*, vol. 59, no. 16, pp. 1384–1390, 2012.
- [15] M. Diouf, A. Ben Salem, R. Cherif, H. Saghaei, and A. Wague, "Super-flat coherent supercontinuum source in As_{388Se}₆₁₂ chalcogenide photonic crystal fiber with all-normal dispersion engineering at a very low input energy," *Appl. Opt.*, vol. 56, no. 2, p. 163, 2017.
- [16] S. Asaduzzaman, K. Ahmed, and T. Bhuiyan, "Design of simple structure gas sensor Based on hybrid photonic crystal fiber," *Cumhur. Üniversitesi Fen-Edebiyat Fakültesi Fen Bilim. Derg.*, vol. 37, no. 3, pp. 187–196, 2016.
- [17] A. M. Fard, M. J. Sarraf, and F. Khatib, "Design and Optimization of Index Guiding Photonic Crystal Fiber-Based Gas Sensor," *Optik (Stuttg.)*, p. 166448, 2021.
- [18] A. Pourfathi Fard, S. Makouei, M. Danishvar, and S. Danishvar, "The Design of a Photonic Crystal Fiber for Hydrogen Cyanide Gas Detection," *Photonics*, vol. 11, no. 2, pp. 178, 2024.
- [19] S. M. Nizar, E. C. Britto, M. Michael, et al., "Photonic crystal fiber sensor structure with vertical and horizontal cladding for the detection of hazardous gases," *Opt. Quant. Electron.*, vol. 55, no. 1186, 2023.
- [20] S. Mortazavi, S. Makouei, and S. M. Garamaleki, "Hollow core photonic crystal fiber based carbon monoxide sensor design applicable for hyperbilirubinemia diagnosis," *Opt. Eng.*, vol. 62, no. 6, pp. 066105, Jun. 27, 2023.

Contribution of Individual Authors to the Creation of a Scientific Article (Ghostwriting Policy)

Zahra Dashtban: Writing – review & editing, Writing – original draft, Visualization, Validation, Software, Methodology, Data curation, Conceptualization, Supervision. Other authors equally contributed in the present research, at all stages from the formulation of the problem to the final findings and solution.

Sources of Funding for Research Presented in a Scientific Article or Scientific Article Itself

No funding was received for conducting this study.

Conflict of Interest

The authors have no conflicts of interest to declare that are relevant to the content of this article.

Creative Commons Attribution License 4.0 (Attribution 4.0 International, CC BY 4.0)

This article is published under the terms of the Creative Commons Attribution License 4.0

https://creativecommons.org/licenses/by/4.0/deed.en_US